Computer simulation of endlinked elastomers. II. Bulk cured tetrafunctional networks

YuKwan Leung and B. E. Eichinger

Citation: J. Chem. Phys. **80**, 3885 (1984); doi: 10.1063/1.447170

View online: http://dx.doi.org/10.1063/1.447170

View Table of Contents: http://jcp.aip.org/resource/1/JCPSA6/v80/i8

Published by the American Institute of Physics.

Computer simulation of end-linked elastomers. II. Bulk cured tetrafunctional networks[a)]

Yu-Kwan Leung
Department of Applied Science, Hong Kong Polytechnic, Hung Hom, Hong Kong

B. E. Eichinger
Department of Chemistry, BG-10, University of Washington, Seattle, Washington 98195

(Received 30 September 1983; accepted 6 January 1984)

Sol–gel distributions at high conversions, simulated by computer with spatial constraints on the distribution of chain ends, are reported for end-linked tetrafunctional systems. The composition of the sol is found to be uniquely dependent upon the functionality f of the cross linker: for $f = 4$, it mainly consists of linear monomers and oligomers containing one saturated cross linker. The molecular weight distribution of the sol exhibits a shoulder at the trimer due to the relative abundance of the "bow-tie" molecule. The populations of various types of dangling ends and loop defects in the gel are given and discussed. Our simulations reveal empirically that the single-loop probability varies with the $-3/8$ power of the molecular weight of the prepolymers. The power-law dependence of the loop formation on chain length of the prepolymers and the nonrandom nature of the cross-linking reaction is discussed.

I. INTRODUCTION

Polymer networks prepared by end-linking primary chains[1–3] have defined structural characteristics which make them useful for the investigation of the quantitative relations of rubber elasticity.[4,5] Detailed information on network structural statistics can be obtained provided that the effects of intramolecular reactions to form cyclics,[6,7] which must occur during cross linking, are properly taken into account. In the preceding paper,[8] we have described a computer simulation experiment to model nonlinear polymerization with inclusion to cyclization, and there we applied the method to trifunctional systems. Detailed description of the sol constituents and the elastic activity of the gel were given. In the present paper, we detail the results of end-linking difunctional primary chains with tetrafunctional cross linkers with use of the same computer scheme. The effect of cross-link functionality on network formation and an analysis of the sol–gel distributions are reported for the tetrafunctional case, and the results are compared with those in the previous paper.

II. PROGRAM

Calculations on telechelic difunctional poly(dimethylsiloxane) and tetrafunctional cross linkers were performed on systems of 10 000 primary chains. Simulations of this size were found to be adequate to represent a macroscopic reaction.[9] The algorithm for end linking was described previously.[8] Experimental results reported here are averages of four runs representing different chain end configurations. At high conversions, only one large particle, whose size is proportional to the weight fraction of the gel, was obtained, which agrees with the results obtained from other approaches.[10,11]

[a)] This work performed at the University of Washington.

III. RESULTS

A. The sol portion

The structures of the sol molecules depend heavily upon the functionality of the cross-linking agent. When cycle formation is allowed in all reactions, different functionalities yield distinctive distributions of sol molecules. The compositions of several constituents of the sol are listed in Table I where w_g and w_x are the weight fractions of the individual graphs and the x-mer, respectively. Results were generated by reacting PDMS oligomers having 50 skeletal bonds to an extent of reaction of 90.6%, yielding a sol fraction of 0.026. The proportion of monomer in the tetrafunctional system is higher than for the trifunctional at similar conversions due to the smaller number of crosslinkers in the tetrafunctional case, which makes the growth of monomer to larger size more difficult.

It can be seen that there are essentially two types of molecules in the sol; these are the linear monomer and those containing one cross linker, all of whose functions are saturated. The latter includes the "butterfly" dimer, the "bow-tie" trimer, and the four-arm star tetramer. The sum of these four accounts for $\sim 96\%$ by weight of the sol. The abundance of molecules with saturated cross linkers is in accordance with the general expectation that the extent of reaction of the cross linker at high conversions will be as large as possible. The weight fraction of the trimer w_3 is greater than that of the dimer w_2. This is attributed to the popularity of the bow-tie trimer.

Aside from its being incorporated into the gel particle, a "tadpole" dimer, consisting of a loop and a chain, may be converted into a bow-tie trimer, a butterfly dimer, or a tadpole trimer, depending upon the route of reaction. When a third chain approaches the tadpole dimer, it will most likely attach itself to the junction of the dimer, at which an unreacted B functional group exists, instead of to the tail of the tadpole because the second route may require an additional

 0021-9606/84/083885-07$02.10

TABLE I. Sol constituents for tetrafunctional systems.[a]

x-mer	graph	$W_g \times 10^2$	$W_x \times 10^2$
1		1.97	2.00
		0.03	
2		0.10	0.16
		0.03	
		0.03	
3		0.24	0.26
		0.01	
		0.01	
4		0.12	0.15[b]

[a] At $P_A = 0.906$ and $n = 50$.
[b] Includes cyclic tetramers.

cross linker which is scarce at high conversion. This results in the favorable formation of the bow-tie trimer. If the tail of the tapole dimer coils up and reacts with the central junction, it will produce the butterfly dimer, an inert species. The butterfly, once formed, will remain unchanged and its number will increase with conversion. The relatively large number of monomers available makes the bow-tie pathway more likely than that leading to the formation of the second loop in the butterfly.

The mole fractions of x-mers N_x are plotted against the extents of reaction in Fig. 1. In the vicinity of 90% conversion, the numbers of dimers and trimers are about the same. In terms of weight fractions, the trimer, which is composed mainly of the bow-tie molecule, outweighs the dimer for p_A greater than ~ 0.70, causing a shoulder in the molecular weight distribution. This deviation from the monotonic distribution that is predicted by the treelike model[12] results from intramolecular reactions that form cyclics. We find that, as far as the sol portion is concerned, $\sim 28\%$ of the total reactions occur intramolecularly at $p_A = 0.906$. The extent of intramolecular reaction is significant in the post-gel period. It is apparent that the sol obtained in a $A_2 + B_f$ copolymerization contains as many cyclics as trees for dimers and up and, therefore, the assumption that the sol structure is treelike[12,13] is not an accurate approximation for describing the distribution of interest for low molecular weight prepolymers.

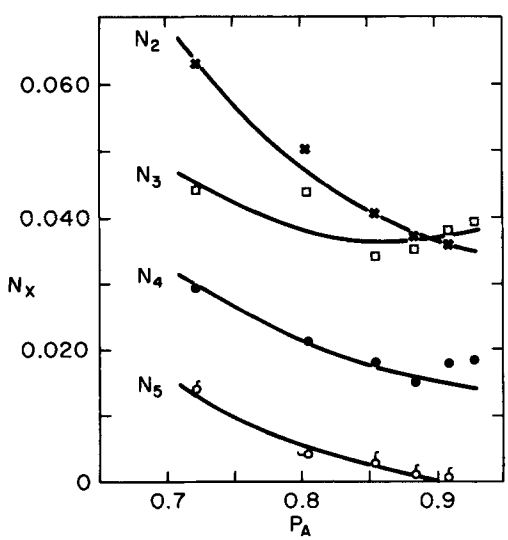

FIG. 1. Variations of the mole fraction of x-mer N_x with the extent of reaction: dimer(×), trimer(□), tetramer(●), and pentamer(σ).

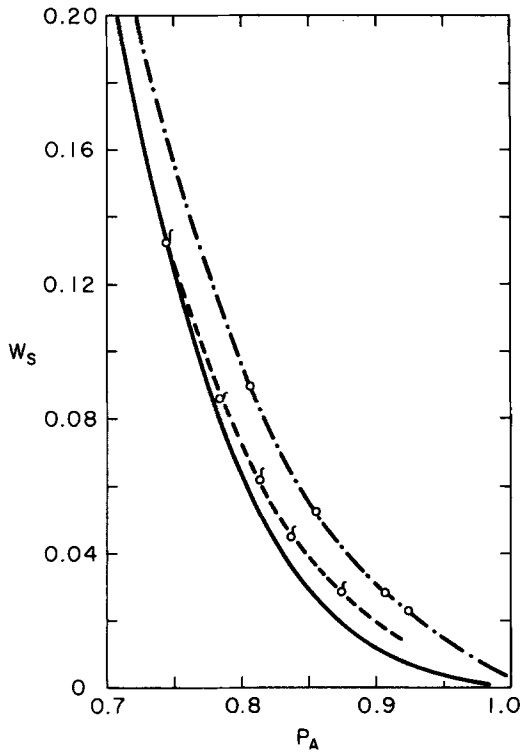

FIG. 2. Plots of sol fraction vs the extent of reaction for tetrafunctional systems: MW = 1850 (○) and 45 000 (σ). Solid curve is drawn according to the branching theory (Ref. 13).

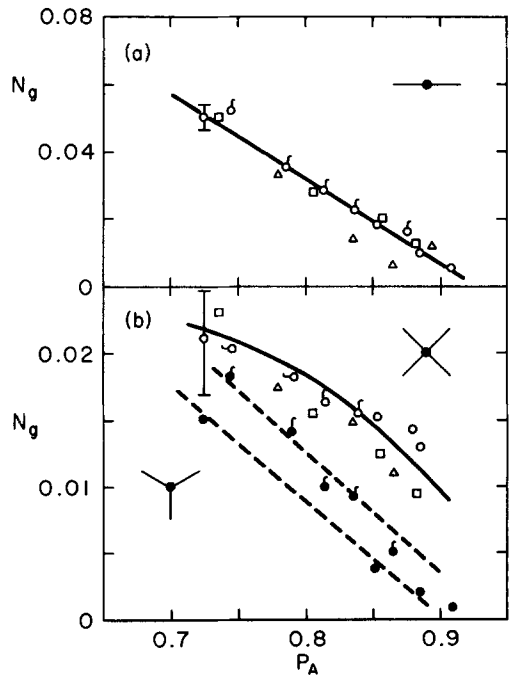

FIG. 3. Mole fractions N_g of linear dimer (a), four-arm star tetramer and three-arm star trimer (b). MW = 1850 (○), 11 400 (△), 18 500 (□), and 45 000 (σ). The open and filled symbols in (b) represent results for the branched tetramer and branched trimer respectively.

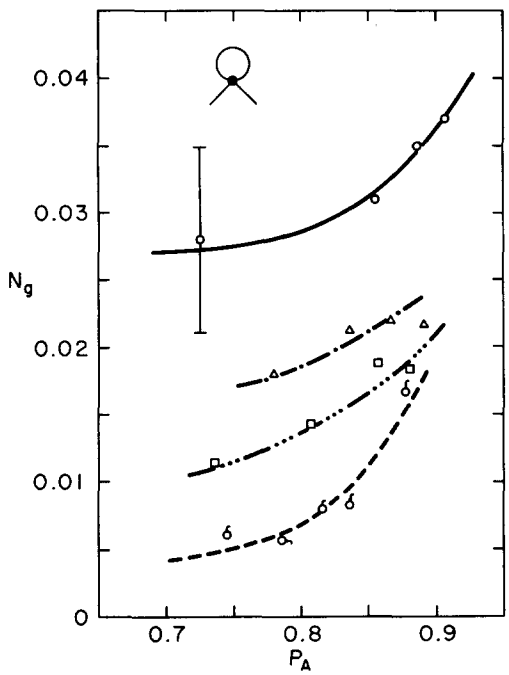

FIG. 4. Mole fractions N_g of the bow-tie trimer. Symbols same as Fig. 3.

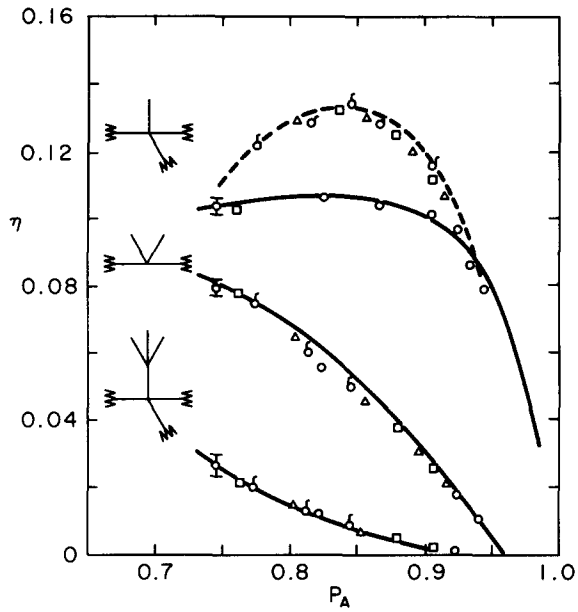

FIG. 5. Populations of I_4, V, and "Ψ" dangling ends. Symbols same as Fig. 3. The broken line represent results of the I_4 ends for $MW>11\,400$.

Variations of sol fractions with conversions are depicted in Fig. 2. Results for MW = 1850 and 45 000 are represented by *circles* and *apples*, respectively, whereas the solid curve was drawn according to the recursion theory of Miller and Macosko.[13] It is noted that at high conversions, neglect of intramolecular reactions underestimates the extent of reaction by as much as 4–6% for molecular weights of the prepolymer in the range of several thousand. The departure from the solid curve is still substantial for high molecular weight prepolymers. These findings are consistent with those obtained for trifunctional systems.

Simulations have been performed for four different molecular weights of PDMS oligomers. Figures 3 and 4 show the trend of the mole fractions N_g of some selected graphs, such as the linear dimer, the three-arm star, the four-arm star, and the bow-tie trimer. Results for MW = 1850, 11 400, 18 500, and 45 000 are given by the *circles*, *triangles*, *squares*, and *apples*, respectively. The same symbols will be used for all stoichiometric systems. The populations of acyclic species decrease with conversions as expected. Of the three acyclic graphs reported here, only the three-arm star shows a slight dependence on molecular weight. On the other hand, the mole fraction of the bow-tie trimer (see Fig. 4) increases with shorter chain lengths and higher extents of reaction. However, extrapolation to complete conversion is not simple because this molecule must eventually be incorporated into the gel. Other cyclic species such as the tadpole dimer and cyclic monomer were found to vary with MW but to be insensitive to the degree of conversion. The mole fraction of the butterfly dimer is on the order of 10^{-4} for molecular weights greater than 10 000 and its presence is only substantial for short primary chains.

B. The structure of the gel

Imperfect networks contain irregularities such as dangling ends and loop defects. Our program can identify five types of dangling ends and two types of loop defects. The population η of each irregularity, expressed in terms of the number of fragments per network chain, is shown in Figs. 5, 6, and 7. These are two different kinds of "I" free ends, one connected to a saturated junction (see Fig. 5) and the other connected to an unsaturated junction (see Fig. 6), which are designated as I_4 and I_3, respectively. The I_4 end is most prevalent at p_A around 0.85. The I_4 configuration is the offspring of its preceding "V" and I_3 structures and therefore its rate of

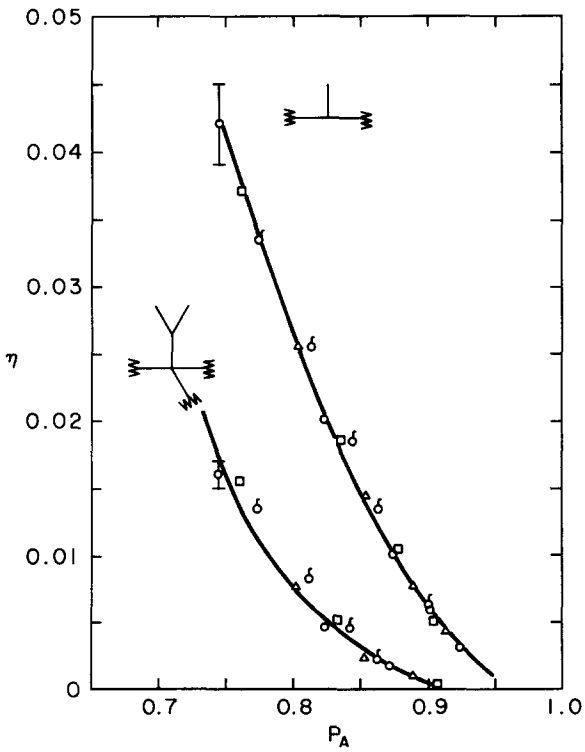

FIG. 6. Populations of I_3 and Y dangling ends. Symbols correspond to those in Fig. 2.

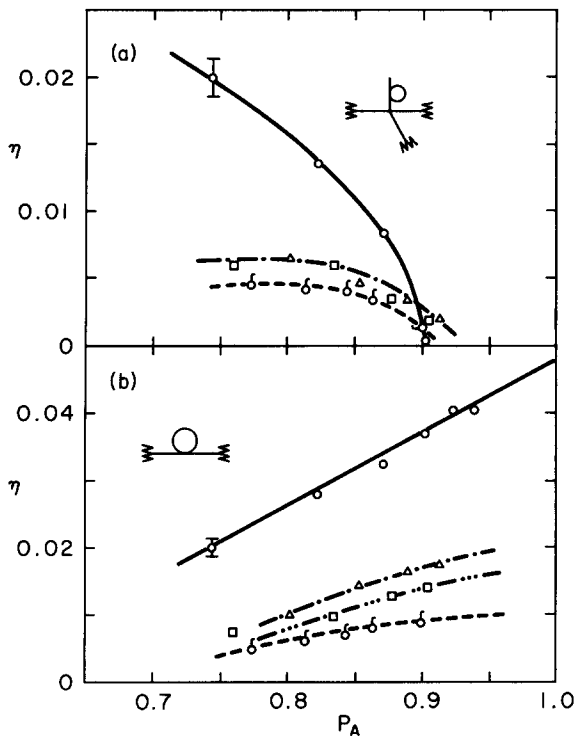

FIG. 7. Variations of dangling loop (a) and inner loop (b) populations with the extents of reaction. Symbols same as Fig. 3.

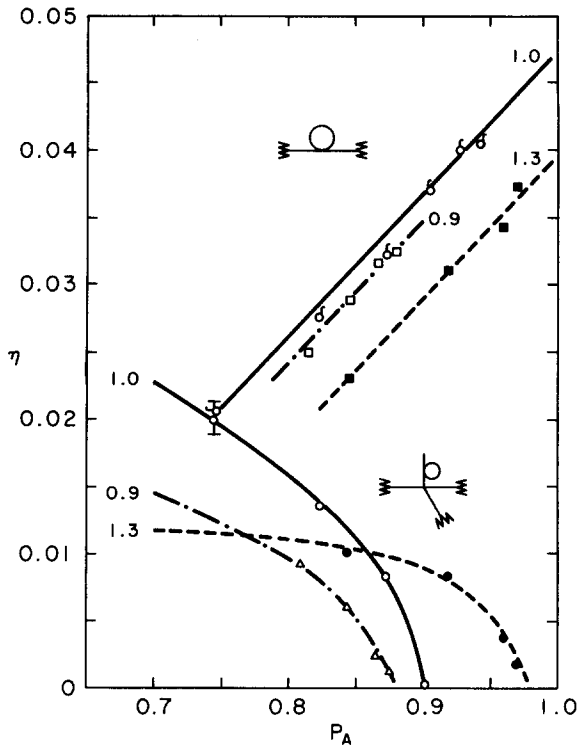

FIG. 8. Plots of dangling loop and inner loop populations for different stoichiometric systems with r values indicated: $r = 1.0$ (solid line), 1.3 (broken line), and 0.9 (dash–dot line).

formation is proportional to the population of the preceding ends. The I_4 free end disappears via attachment to another part of the network. It seems that for p_A below 0.85, the formation rate exceeds the rate of disappearance, resulting in a net gain in the I_4 ends, but the reverse is true for p_a higher than 0.85. Other types of unattached ends decrease monotonically with conversion. Also, the population of I_4 is less for low molecular weight prepolymers. The decrease in I_4 is consistent with the tendency for I_3 of the short chains to form more loops, thus reducing the chance of conversion to I_4. However, for sufficient long chains, e.g., $n > 300$, I_4 does not show a molecular weight dependence.

Dangling loops [see Fig. 7(a)] vanish as they are converted into the inner loop structure [see Fig. 7(b)] as cross linking proceeds to over 90% completion. But the inner loops are stable and their number increases with shorter chains and with higher extents of reaction. It can be seen that networks formed with less than about 5% unreacted functional groups contain only the I_4 and inner loop defects.

Various defects in networks produced by using different stoichiometric ratios r, defined as the ratio of the numbers of B to A groups, are shown in Figs. 8, 9, and 10. The solid, broken, and dash–dot curves drawn in those figures represent results obtained at $r = 1.0$, 1.3, and 0.9, respectively. For nonstoichiometric systems, structural irregularities for the final networks obtained at complete reaction of the least abundant functional group include dangling ends in addition to the inner loop defects. The cycle rank per chain (ξ/ν) for the various networks are shown in Fig. 11. At complete conversion, the stoichiometric network has the highest cycle rank value of ~ 0.48, which is 4% less than the theoretical value obtained for a perfect tetrafunctional network. The imperfection of this network arises from the presence of inner loops which are elastically inactive. Cross-link deficient mixtures would produce less effective elastic networks than those using excess cross linkers. This can be illustrated by noting that networks prepared by using $r = 0.9$ and 1.3 have approximately the same cycle rank values. However, the former is only 10% deficient in B groups, while the latter departs from stoichiometric balance by 30%. At complete reaction, both I_4 and V dangling ends exist in

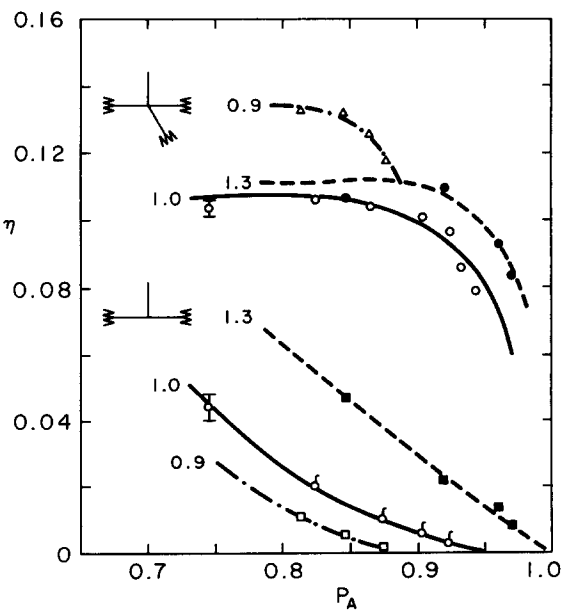

FIG. 9. Plots of I_4 and I_3 populations obtained at different stoichiometric ratios r. Line symbols used are same as Fig. 8.

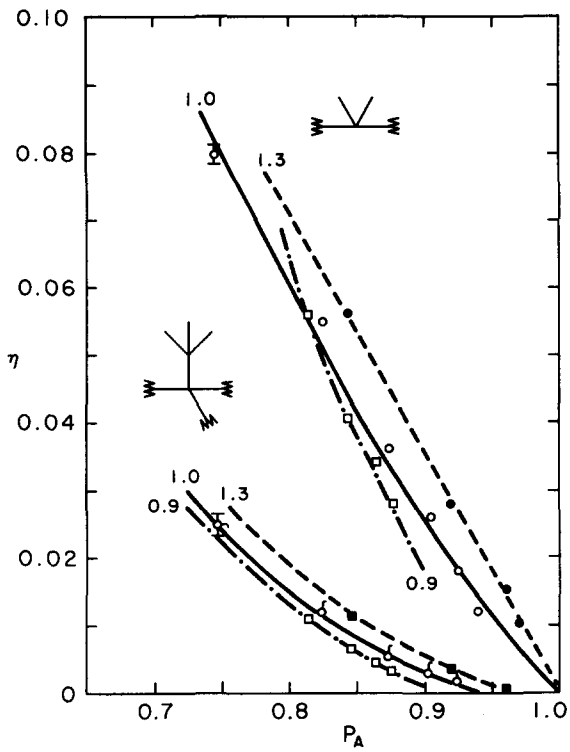

FIG. 10. Variations of the V and Ψ dangling ends populations for different stoichiometric systems. Line symbols correspond to those in Fig. 8.

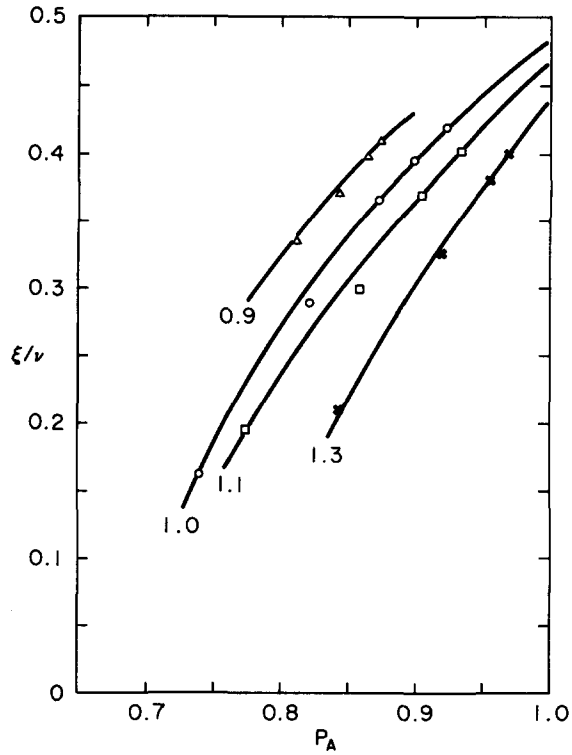

FIG. 11. The cycle rank per chain of the tetrafunctional end-linked elastomers obtained at different extents of reaction and different stoichiometric ratios: $r = 0.9$ (△), 1.0 (○), 1.1 (□) and 1.3 (×). The primary chain has 50 skeletal bonds.

the $r = 0.9$ network, whereas only the I_4 type is found for the $r = 1.3$ network.

C. Variation of single-chain loops with chain lengths

In these computer simulations, we find that the population of single-chain loops increases with decreasing MW of the primary chains. The single-loop probability is here expressed as the weight function η_0 of the prepolymers whose ends are connected to each other. Assuming a power-law dependence of η_0 on molecular weight, we made log–log plots of η_0 vs mean-square end-to-end distance $\langle r^2 \rangle_0$ of the prepolymer at fixed extent of reaction. Four sets of data were compiled for the following values of (f, p_A): (3,0.80), (4,0.80), (3,0.90), and (4,0.90). A least squares fit of the data points gives parallel straight lines with an average slope of -0.38 and standard deviation of 0.02, which shows that the power-law relationship is valid for the stated range of investigation. For convenience, an exponent of $-3/8$ is taken for subsequent calculations. The results are recast in Fig. 12 where the

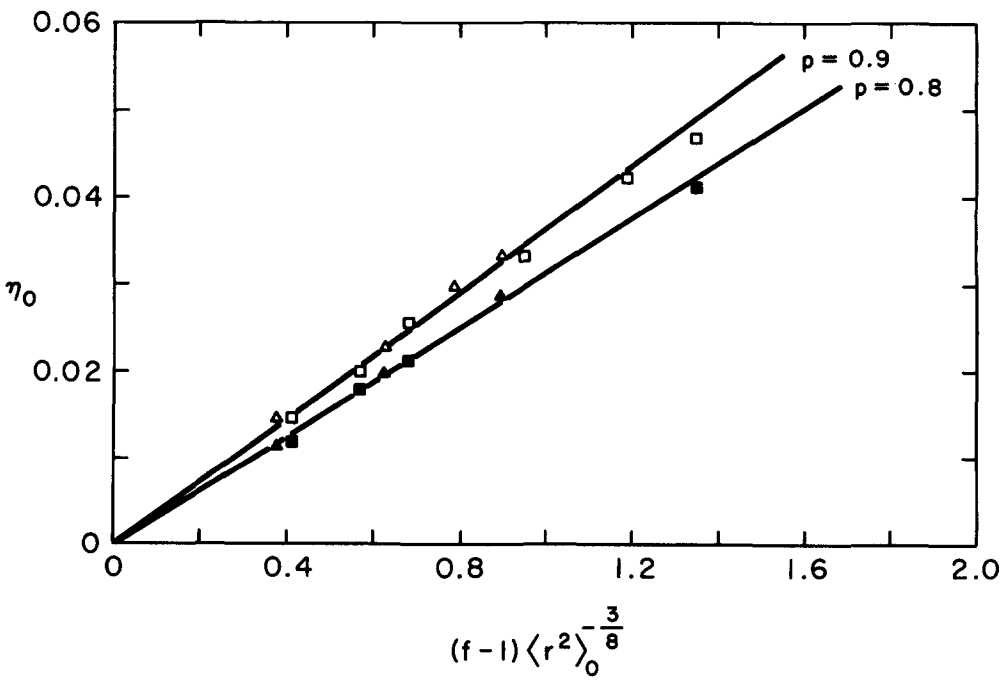

FIG. 12. Plots of the weight fraction η_0 of one-chain loops vs $(f-1)\langle r^2 \rangle_0^{-3/8}$. The filled triangles and squares represent systems with $f = 3$ and 4, respectively, for $P_A = 0.80$, whereas the open symbols represent similar quantities for $P_A = 0.90$.

values of η_0 are plotted against $(f-1)\langle r^2\rangle_0^{-3/8}$. From these results, it is found that at the same extent of reaction, the single-loop probability varies with the number of skeletal bonds n of the primary chains according to

$$\eta_0 = k(f-1)\langle r^2\rangle_0^{-3/8} = k'(f-1)n^{-3/8}. \quad (1)$$

The factor k (or k') is observed to be roughly proportional to the extent of reaction.

IV. DISCUSSION

Some of the results given above are susceptible to analysis. We have shown that the sol distributions obtained are distinctly different from those predicted by branching theory.[12,13] Since other methods which consider the effect of intramolecular reaction seldom extend to cover the post-gel region, quantiative comparison of the sol–gel distributions among various methods cannot now be made. However, the overall probability of single-loop formation, as revealed by Eq. (1), will be discussed in detail.

Suppose the end-to-end distance of a primary chain is between r and $r+dr$. It will react to form a loop if no other ends exist within a sphere of radius r and the reacting ends are within the cross-linking distance d of each other. The value d is set in the program such that groups which are more than the distance d apart do not have a chance to react. Here, to a first approximation, we neglect the role of the cross linker in the loop formation reaction. Thus, the probability of forming a single-loop $P_l(n)$ as a function of n is given by the product of two independent factors: the first gives the probability that there is not another end within a sphere of radius r, and the second gives the probability that the other end of the given chain is within the shell from r to $r+dr$, with $r<d$. This must then be integrated from $r=0$ to $r=d$, to give

$$P_l(n) = \int_0^d \left(\frac{\beta}{\pi^{1/2}}\right)^3 \exp(-\beta^2 r^2) W(n,r) 4\pi r^2\, dr, \quad (2)$$

where $W(n,r)$ is the probability that no chain ends exist interior to r and the term $(\beta/\pi^{1/2})^2\exp(-\beta^2 r^2)$ is the Gaussian density distribution of the chain displacement vector with the parameter β^2 given by $3/2\langle r\rangle_0^2$. Equation (2) is similar to the Jacobson–Stockmayer ring–chain factor.[14] The expression for $W(n,r)$ is given[15] by

$$W(n,r) = 1 - \int_0^r w(n,r) 4\pi r^2 \rho_0\, dr = \exp(-4\pi r^3\rho_0/3), \quad (3)$$

where ρ_0 denotes the average number of chain ends per unit volume and $w(n,r)4\pi r^2\rho_0\, dr$ is the density distribution of the nearest neighbor in a random distribution of chain ends. The chain end density ρ_0 can be determined from

$$\rho_0 = 2cN_a/nM_0, \quad (4)$$

where c is the weight of the prepolymer per unit volume, M_0 is the molecular weight of one bond unit, and N_a is Avogadro's number. For elastomers cured in the bulk, c is equal to the density of the prepolymer. Numerical integrations of the single-loop probability function Eq. (2) were carried out for different n ranging from 50 to 1216. To further simplify the problem, a large d was chosen so that results of the integration approach the asymptotic value obtained at complete conversion. The unnormalized probabilities thus calculated are 0.2094, 0.1031, 0.0841, and 0.0571 for $n=50$, 308, 500, and 1216, respectively. It is found that the dependence of $P_l(n)$ upon n may be expressed as

$$P_l(n) = K'' n^{-0.406}. \quad (5)$$

The exponent -0.406 is very close to that determined from the computer simulation. The discrepancy between the two powers in Eqs. (1) and (5), which is about 10%, may be attributed to complications arising from the participation of the cross linker in the loop formation process.

Recently, Roovers and Toporowski[16] synthesized single-chain cyclic polystyrenes by reacting two-ended living polystyrylsodium with dimethyldichlorosilane. Their nearly "monodisperse" samples make quantitative determination of the ring fraction possible. They used a consecutive addition procedure which is different from the batch model employed in our computer simulation. A least squares fit of the ring fraction data for their A-series data[17] gives an exponent of -0.29 as the power law in the ring fraction-molecular weight relation. This result is compatible with our finding for the batch reaction, though the comparison can only be viewed as qualitative due to the different procedures of addition.

In our model, reaction does not occur at random, but centers on the cross-linking unit whose sphere of reaction has the volume $4\pi d^3/3$.[8,17] This is reflected in the distribution of the numbers of the cross linkers of degree i. For example, in random reactions, the probability of finding a cross linker of degree i, denoted by P_{ic}, is given by the $(i+1)$ term in the polynomial $[(1-P_A)+P_A]^f$. The P_{2c}, P_{3c}, and P_{4c} values obtained from the computer experiment at an extent of reaction $p_A = 0.45$ are found to be 0.256, 0.164, and 0.133, respectively, which depart significantly from 0.367, 0.20, and 0.04 calculated from the random hypothesis. The random reaction underestimates the occurrence of saturated cross linkers at high conversion.

The other extreme is the "target" model. In the target model, a cross linker will have saturated degree if the sphere of reaction ascribed to it encloses more than $(f-1)$ chain ends. In N attempts, the probability $P(n)$ that n chain ends distributed at random will land inside the reaction sphere is

$$P(n) = \binom{N}{n}\alpha^n(1-\alpha)^{N-n} = \frac{(N\alpha)^n}{n!}e^{-N\alpha} \quad \text{for } n \ll N, \quad (6)$$

where α is the volume percentage occupied by one sphere of reaction and $\binom{N}{n}$ is the binomial coefficient. For $i \leqslant 3$, $P_{ic} = P(i)$ and for $i=4$,

$$P_{4c} = \sum_{n=4}^{\infty} P(n) = 1 - \sum_{n=1}^{3} P(n). \quad (7)$$

This model assumes that spheres of reaction are isolated from one another and hence that competition between neighboring cross linkers for chain ends does not occur. Such a model will only give reasonable predictions for P_{ic} when $P_A < 0.45$, where the spheres assigned to the cross linkers start to overlap each other. The values found for the three probabilities are 0.25, 0.22, and 0.27, respectively. It

can be seen that the computer results for P_{4c} lie between the random and the target models. The assumption of isolated cross linkers overestimates the probability for cross linkers of highest degree: for higher extents of reaction, the target model is not applicable because the competition for chain ends by neighboring cross linkers will be profound and cannot be neglected. In fact, cross linking in the post-gel region in real systems cannot be considered to be a random reaction because the dangling ends of the gel particle have a limited range of access to other reactive groups: only the sol molecules can move freely about in the reaction vessel. The restricted movement of the dangling ends renders the hypothesis of random reaction inappropriate near and beyond the gel point of the nonlinear polymerization. While a complete theoretical approach is not possible at present, computer simulations of this kind provide a reasonable means to tackle this complicated problem. If the cross-linking distance d is thought to be analogous to the average distance the end has traveled from its time-average position before it is reacted, then the simulation described here may be considered, in some way, as a time-dependent diffusion-controlled process.

V. CONCLUSION

Sol structures are very much dependent upon the functionality of the cross linkers used in the end-linking process. Intramolecular reactions which occur in substantial proportion at the later stages of the polymerization necessarily favor formation of cyclic species. In the case of tetrafunctional systems, this results in a nonmonotonic molecular weight distribution of the sol constituents. Derivation of the extent of reaction from sol fractions alone is not accurate if cyclic molecules are disallowed as is postulated in branching theory. Tetrafunctional networks obtained at complete conversion are found to contain some single-chain loop defects: for very low chain lengths, e.g., $n = 50$, the elastic activity is about 4% below that predicted for the perfect network. Given the general magnitude of the deficit of chains due to intramolecular reactions, it seems that networks obtained near complete conversions are fairly close to perfect,[18,19] so that the chain entanglement term is less important than has been postulated.[3,20]

ACKNOWLEDGMENT

This work was supported by the Department of Energy, contract DE-AT06-81EF10912.

[1] J. E. Mark and J. L. Sullivan, J. Chem. Phys. **66**, 1006 (1977); J. E. Mark and P.-H. Sung, J. Eur. Polym. J. **16**, 1223 (1980).
[2] E. M. Valles and C. W. Macosko, Macromolecules **12**, 521 (1979).
[3] K. O. Meyers, M. L. Bye, and E. W. Merrill, Macromolecules **13**, 1045 (1980).
[4] P. J. Flory, Proc. R. Soc. London. Ser. A **351**, 351 (1976).
[5] W. W. Graesley, Macromolecules **8**, 186, 865 (1975).
[6] M. Falk and R. E. Thomas, Can. J. Chem. **52**, 3285 (1974).
[7] J. L. Stanford, R. F. T. Stepto, and D. R. Waywell, J. Chem. Soc. Faraday Trans. 1 71, 1308 (1975).
[8] Y. K. Leung and B. E. Eichinger, J. Chem.Phys. **80**, 3878 (1984).
[9] Y. K. Leung and B. E. Eichinger, in *Characterization of Highly Cross-linked Polymers*, edited by S. S. Labana and R. A. Dickie, ACS Symposium Series (American Chemical Society, Washington, D.C., 1984), Vol. 243, p. 21.
[10] J. Mikeš and K. Dušek, Macromolecules **15**, 93 (1982).
[11] E. Donoghue, J. Chem. Phys. **77**, 4234 (1982); Macromolecules **15**, 1634 (1982).
[12] P. J. Flory, *Principles of Polymer Chemistry* (Cornell University, Ithaca, 1962), Chap. 9.
[13] D. R. Miller and C. W. Macosko, Macromolecules **9**, 206 (1976).
[14] H. Jacobson and W. H. Stockmayer, J. Chem. Phys. **18**, 1600 (1950).
[15] S. Chandrasekhar, in *Selected Papers on Noise and Stochastic Processes*, edtied by Nelson Wax (Dover, New York, 1954), p. 88.
[16] J. Roovers and P. M. Toporowski, Macromolecules **16**, 843 (1983).
[17] B. E. Eichinger, J. Chem. Phys. **75**, 1964 (1981).
[18] P.-H. Sung and J. E. Mark, J. Polym. Sci., Polym. Phys. Ed. **19**, 507 (1981).
[19] P.-H. Sung, S.-J. Pan, J. E. Mark, V. S. C. Chang, J. E. Lackey, and J. P. Kennedy (unpublished).
[20] M. Gottlieb, C. W. Macosko, G. S. Benjamin, K. O. Meyers, and E. W. Merrill, Macromolecules **14**, 1039 (1981).